Title

Role of Pyridoxal 5′-Phosphate in the Structural Stabilization of O-Acetylserine Sulfhydrylase*

Journal

Journal of Biological Chemistry, 275(51)

ISSN

0021-9258

Authors

Bettati, Stefano
Benci, Sara
Campanini, Barbara
et al.

Publication Date

2000-12-01

DOI

10.1074/jbc.m007015200

THE JOURNAL OF BIOLOGICAL CHEMISTRY
Vol. 275, No. 51, Issue of December 22, pp. 40244–40251, 2000
Printed in U.S.A.

Role of Pyridoxal 5′-Phosphate in the Structural Stabilization of *O*-Acetylserine Sulfhydrylase*

Received for publication, August 3, 2000, and in revised form, September 11, 2000
Published, JBC Papers in Press, September 19, 2000, DOI 10.1074/jbc.M007015200

Stefano Bettati‡§¶, Sara Benci‡¶, Barbara Campanini§, Samanta Raboni§, Giuseppe Chirico‖, Sabrina Beretta‖, Klaus D. Schnackerz, Theodore L. Hazlett‡‡§§, Enrico Gratton‡‡§§, and Andrea Mozzarelli§¶ ¶¶**

*From the ‡Institute of Physical Sciences, §Institute of Biochemical Sciences, and ¶National Institute for the Physics of Matter, University of Parma, Parma 43100, Italy, ‖Department of Physics, University of Milan La Bicocca, Milan 20133, Italy, **School of Chemistry, The University of Birmingham, Edgbaston, Birmingham B15 2TT, United Kingdom, and ‡‡Laboratory of Fluorescence Dynamics, University of Illinois at Urbana-Champaign, Urbana, Illinois 61801*

Proteins belonging to the superfamily of pyridoxal 5′-phosphate-dependent enzymes are currently classified into three functional groups and five distinct structural fold types. The variation within this enzyme group creates an ideal system to investigate the relationships among amino acid sequences, folding pathways, and enzymatic functions. The number of known three-dimensional structures of pyridoxal 5′-phosphate-dependent enzymes is rapidly increasing, but only for relatively few have the folding mechanisms been characterized in detail. The dimeric *O*-acetylserine sulfhydrylase from *Salmonella typhimurium* belongs to the β-family and fold type II group. Here we report the guanidine hydrochloride-induced unfolding of the apo- and holoprotein, investigated using a variety of spectroscopic techniques. Data from absorption, fluorescence, circular dichroism, ^{31}P nuclear magnetic resonance, time-resolved fluorescence anisotropy, and photon correlation spectroscopy indicate that the *O*-acetylserine sulfhydrylase undergoes extensive disruption of native secondary and tertiary structure before monomerization. Also, we have observed that the holo-*O*-acetylserine sulfhydrylase exhibits a greater conformational stability than the apoenzyme form. The data are discussed in light of the fact that the role of the coenzyme in structural stabilization varies among the pyridoxal 5′-phosphate-dependent enzymes and does not seem to be linked to the particular enzyme fold type.

Pyridoxal 5′-phosphate (PLP)[1]-dependent enzymes have been classified into the α, β, and γ families based on the chemical characteristics of their enzymatic activities (1). This enzyme group has also been organized on the basis of sequence and structural features, into five distinct fold types (2). Three-dimensional structures have been reported for about 30 PLP-dependent enzymes (3), and the folding mechanism has been investigated in some detail for less than a dozen. Much of the reported data has mainly derived from research on the fold type I enzymes.

Tryptophan synthase, threonine deaminase, and *O*-acetylserine sulfhydrylase (OASS) belong to the β-family and fold type II. These enzymes catalyze β-replacement and/or β-elimination reactions, sharing similar catalytic pathways. Despite the fact that OASS and the β_2 dimer of tryptophan synthase from *Salmonella typhimurium* exhibit closely related reaction mechanisms and a common folding pattern (4, 5), the sequence identity is small, only 20%. A detailed investigation into the folding mechanism of the PLP-dependent enzymes belonging to the same or different families can provide a rare opportunity to uncover the specific structure and function determinants encoded in the primary sequence.

The biosynthesis of L-cysteine from L-serine in bacteria and plants is catalyzed via a two-step process by the multienzyme complex cysteine synthetase (6, 7). Serine *O*-acetyltransferase catalyzes the first step, the acetylation of the β-hydroxyl of L-serine using acetyl-CoA as the acetyl donor. The PLP-dependent OASS catalyzes the synthesis of L-cysteine from *O*-acetylserine and sulfide via a β-replacement reaction (8). The multienzyme complex is composed of two dimers of OASS and two trimers of serine *O*-acetyltransferase (7, 9, 10). In the presence of *O*-acetylserine or other ligands of either of the two enzymes, the complex can be reversibly resolved into the active component enzymes (7, 9, 11).

OASS from *S. typhimurium* is a homodimer (34,450 Da/protomer). Along the catalytic pathway, the coenzyme forms several intermediates. In the absence of substrates or products, PLP is covalently bound via a Schiff base to the ε-amino group of Lys-41 (12). The internal aldimine (13) exists as an equilibrium of enolimine and ketoenamine tautomers with absorption maxima at 330 and 412 nm, respectively (8, 14). The three-dimensional structure of the A-isozyme of OASS from *S. typhimurium* (EC 4.2.99.8) has been recently determined at 2.2 Å resolution (5, 15), and the catalytic competence of the enzyme in the crystalline state has been assessed by polarized absorption microspectrophotometry (16). The active site is localized at the junction between the N- and C-terminal domains. Each protomer contains two tryptophan residues (Trp-50 and Trp-161). Both tryptophans are located about 20 Å apart from the PLP (Fig. 1) (5). The conformational properties of OASS have been investigated in the presence and absence of bound PLP and during the catalytic reaction by measuring the steady-

* The work was supported by Italian University and Scientific and Technological Research Ministry Grant PRIN99 (to A. M.), National Research Council Grant 98.01117.CT14/115.19978 (to A. M.), and National Institutes for the Physics of Matter (to S. B.). The costs of publication of this article were defrayed in part by the payment of page charges. This article must therefore be hereby marked "*advertisement*" in accordance with 18 U.S.C. Section 1734 solely to indicate this fact.

§§ Supported through the National Institutes of Health Grant RR03155.

¶¶ To whom correspondence should be addressed: Institute of Biochemical Sciences, University of Parma, 43100 Parma, Italy. Tel.: 39-0521-905138; Fax: 39-0521-905151; E-mail: biochim@unipr.it.

[1] The abbreviations used are: PLP, pyridoxal 5′-phosphate; OASS, *O*-acetylserine sulfhydrylase; GdnHCl, guanidinium hydrochloride; Bis-Tris propane, Bis-tris[bis-(2-hydroxyethyl)imino]-tris[(hydroxymethyl)propane]; NMR, nuclear magnetic resonance; MES, 2-(*N*-morpholino)ethanesulphonic acid.

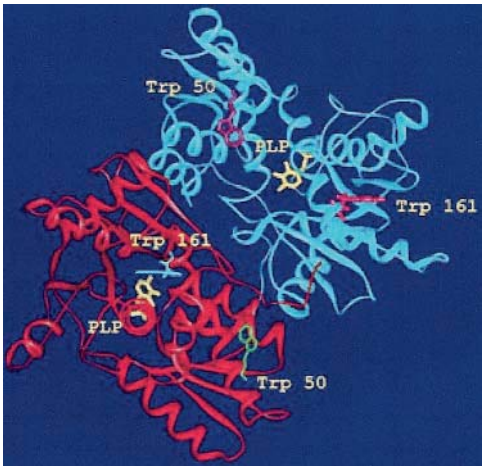

FIG. 1. **Three-dimensional structure of the holo-OASS A-isozyme dimer (PDB file 1OAS).** The coenzyme, Trp-50 and Trp-161, shown in stick mode, are labeled. Both tryptophans belong to α-helical motives (5).

state and time-resolved fluorescence and phosphorescence of the coenzyme and tryptophan residues (17–21). A large conformational change takes place upon ligand binding (14, 15, 19), indicating that some regions of the protein are quite flexible. The comparison of the emission properties of apo- and holoenzyme indicates the presence of an energy transfer between tryptophans and the coenzyme (18, 21). Due to the different orientation of tryptophans transition dipoles, the energy transfer predominantly occurs between Trp-50 and PLP (21).

The presence of multiple intrinsic fluorescent probes allows one to monitor the conformational state of several distinct regions of the protein during the unfolding process and to evaluate the role of the coenzyme in the stabilization of the protein. Here we present data on the guanidine hydrochloride unfolding of OASS. UV-visible absorption spectra, circular dichroism spectra, steady-state and time-resolved fluorescence of PLP and tryptophan, dynamic light scattering, and ^{31}P nuclear magnetic resonance of apo- and holo-OASS were all measured as a function of guanidine hydrochloride concentration.

MATERIALS AND METHODS

Enzyme—The A-isozyme of *O*-acetylserine sulfhydrylase, obtained from a plasmid-containing *S. typhimurium*-overproducing strain (LT-2) according to the method of Hara *et al.* (22), modified by Tai *et al.* (23), was a kind gift of Dr. Paul F. Cook (Department of Chemistry and Biochemistry, University of Oklahoma, Norman, OK). The protein concentration (protomers) was estimated on the basis of an extinction coefficient of 7,600 M^{-1} cm^{-1} at 412 nm (8). The apoenzyme was prepared by extensive dialysis against a solution containing 5 M GdnHCl, 100 mM MES, 10 mM *O*-acetylserine, 0.1 mM dithiothreitol, pH 6.5, at 4 °C, followed by dialysis against 100 mM potassium phosphate, 0.1 mM dithiothreitol, pH 7.0 (24). The concentration was determined by the Bradford method (25). Using the holoenzyme to obtain a calibration curve, an extinction coefficient of 20,000 M^{-1} cm^{-1} (protomers) at 280 nm was obtained for the apoenzyme.

Chemicals—K^+-Hepes, MES, Bis-Tris propane, guanidine hydrochloride, *O*-acetyl-L-serine, fluorescein (Sigma), PLP (Roche Molecular Biochemicals), valine methyl ester and dithiothreitol (Fluka), and *p*-terphenyl (Aldrich) were of the best commercially available quality and were used without further purification.

Buffers—Absorbance, dynamic light scattering, and fluorescence experiments were carried out in a buffer solution containing 100 mM K^+-Hepes, pH 7.0, and variable concentrations of GdnHCl at 20 °C. PLP, PLP-valine methyl ester, and holo-OASS were dissolved in 100 mM Bis-Tris propane, pH 7.0 for ^{31}P NMR spectra. For CD measurements, buffer solutions containing 20 mM potassium phosphate, pH 7.0, were used. Denaturant-containing solutions were prepared according to Pace (26), and GdnHCl concentration was checked by measuring the solution refractive index.

Absorption and Steady-state Fluorescence Measurements—The unfolding rate is strongly dependent on the denaturant concentration and ranged from several minutes to several hours. Therefore, each sample was incubated in GdnHCl solutions for at least 24 h at 20 °C. Absorption spectra were recorded using a Cary 219 spectrophotometer. Fluorescence spectra were collected on a PerkinElmer LS50B fluorometer. Absorption and fluorescence spectra were corrected for solvent contribution. Samples were equilibrated at 20 ± 0.5 °C.

Far UV Circular Dichroism Measurements—Circular dichroism measurements were carried out using a JASCO J-715 spectropolarimeter. The samples were maintained at 20 ± 0.5 °C. Each reported spectrum is the average of three measurements. Fractions of α and β structure were calculated by deconvoluting the observed spectra with the CD Spectra Deconvolution software (65).

Equilibrium Analysis—The thermodynamic parameters of the transition between the native and the unfolded states of holo- and apoenzyme were determined from steady-state fluorescence and circular dichroism equilibrium curves by the linear extrapolation method (26), according to a two-state model.

The equilibrium unfolding constants K_U at each denaturant concentration were calculated from the equation,

$$K_U = \frac{f_U}{1 - f_U} \qquad \text{(Eq. 1)}$$

where f_U is the fraction of unfolded protein, calculated as,

$$f_U = \frac{I - I_{0,N}}{(I_{0,U} + S_U[\mathrm{D}]) - I_{0,N}} \qquad \text{(Eq. 2)}$$

where I and $I_{0,N}$ are the observed signal intensity at a defined denaturant concentration and in the absence of denaturant, respectively; $I_{0,U}$ is the extrapolated intensity of the fully denatured species, S_U is the post-transition slope, and [D] is the denaturant concentration.

The K_U values were used to calculate the unfolding free energies as follows.

$$\Delta G^0_U = -RT \ln K_U \qquad \text{(Eq. 3)}$$

$\Delta G^0_{0,U}$, the free energy change in the absence of denaturant, and m, the dependence of ΔG^0_U on denaturant concentration, were calculated using the following equation.

$$\Delta G^0_U = \Delta G^0_{0U} - m[\mathrm{D}] \qquad \text{(Eq. 4)}$$

By combining Equations 1–4, the following is obtained.

$$I = \frac{I_{0,N} + (I_{0,U} + S_U[\mathrm{D}])e^{\frac{-\Delta G^0_{0,U} + m[\mathrm{D}]}{RT}}}{1 + e^{\frac{-\Delta G^0_{0,U} + m[\mathrm{D}]}{RT}}} \qquad \text{(Eq. 5)}$$

Time-resolved Fluorescence Measurements—Fluorescence intensity decays were measured by the phase and modulation technique and were fitted to a sum of discrete exponentials by the Marquardt algorithm of the Globals Unlimited software (University of Illinois, Urbana, IL) (27). Tryptophan fluorescence lifetimes were measured at a protomer concentration of 9.65 and 4.80 μM for the holoenzyme and the apoenzyme, respectively and will be reported in detail elsewhere.[2] The modulated 295-nm excitation light was obtained from the output of a frequency-doubled, cavity-dumped rhodamine dye laser (Coherent, model 700) synchronously pumped by a Coherent Antares Nd/YAG laser. The emission was collected through a Schott WG320 cut-off filter in order to eliminate scattering of the excitation light by the sample. Modulated excitation light at 454.5 nm was obtained using a Spectra Physics model 2017 Argon-ion laser modulated through a Pockel cell on an ISS Instruments phase and modulation fluorometer. The fluorescence was collected through a Hoya Y48 filter to eliminate scatter of the excitation light. In these experiments the holoenzyme concentration was 19.3 μM protomers. A *p*-terphenyl solution in ethanol (1.05 ns) or a fluorescein solution in diluted NaOH (4.05 ns) were used as lifetime standard references for excitation at 295 and 454.5 nm, respectively. Rotational correlation times were calculated from the differential polarized phase and the modulation ratio between the perpendicular and parallel components of the emission across a modulation range from 2–250 MHz (28, 29). Optical filters used in the emission path were identical to those used in the fluorescence lifetime experiments above.

[2] S. Bettati, S. Benci, B. Campanini, G. Schianchi, S. Vaccari, T. L. Hazlett, E. Gratton, and A. Mozzarelli, manuscript in preparation.

Differential phase and modulation data were analyzed using the Globals Unlimited software with standard errors of 0.2° and 0.01 for the differential phase and modulation, respectively. Data were well fitted to a double exponential decay model.

Photon Correlation Spectroscopy—The laser source at 532 nm for the photon correlation spectroscopy apparatus was a frequency doubled Nd:YVO_4 (1064 nm) diode-pumped laser (Millennia II, Spectra Physics) in TEM_{00} mode. The beam was spatially filtered and focused at the center of a 10-mm square quartz cell with a sample volume of about 400 μl. Two replicas of the scattered light were detected by two photomultipliers tubes (H5873P-01, Hamamatsu), and the discriminated signals were sent to the two inputs of an ALV5000E/fast digital correlator (ALV, Germany) for the computation of the pseudo-cross-correlation functions. Further details of this set-up can be found elsewhere (30).

The measurements were performed at a 90° scattering angle with a laser power of about 1 W at 24.5 °C. The protein concentration was 35–45 μM, and sample solutions were filtered with 0.2-μm low protein adsorption filters (Nucleopore).

The auto-correlation function of the intensity of the scattered light was analyzed as an exponential decay with relaxation rate $\Gamma = Dq^3$, related to the protein mutual diffusion coefficient D and to the scattering vector q. The dependence of q on the solution refractive index n, vacuum wavelength λ, and scattering angle θ was taken into account according to the relation $q = 4\pi n \sin(\theta/2)/\lambda$. The hydrodynamic radius of the protein, a, was obtained from the diffusion coefficient D by the Stokes-Einstein relation,

$$D = \frac{k_B T}{6\pi\eta a} \qquad \text{(Eq. 6)}$$

where k_B is the Boltzmann's constant, T is the absolute temperature, and η is the solvent viscosity. The refractive index of the solutions required for the computation of the scattering vector q was measured by an Abbe refractometer to three significant digits and cross-checked with values obtained from the literature (31). The solution viscosity, η, necessary for the computation of the protein radius from the diffusion coefficient, was assumed to be equal to that of the solvent and was obtained from the literature (32).

NMR Measurements—Fourier transform ^{31}P NMR spectra were collected at 121.496 MHz on a Bruker 300 MHz SWB superconducting spectrometer using a 10-mm multinuclear probe head with broadband ^1H decoupling. The NMR tube, containing the sample (2 ml) and ^2H_2O (0.2 ml) as field/frequency lock, was maintained at 20.0 ± 0.1 °C using a thermostated air flow. A solution containing OASS (15 mg/ml), 100 mM Bis-Tris propane, pH 7.0, was used. A spectral width of 2000 Hz was acquired in 8192 data points with a pulse angle of 60°. The exponential line broadening used before Fourier transformation was 10 Hz. Positive chemical shifts in ppm are downfield changes with respect to 85% H_3PO_4. The ^{31}P NMR spectra were collected in less than 5 h using protein concentrations high enough to assure a ^{31}P signal with a reasonable signal to noise ratio.

RESULTS

UV-Visible Absorption and Steady-state Fluorescence Spectra of OASS as a Function of GdnHCl Concentration—The internal aldimine of OASS exhibited an absorption band centered at 412 nm (Fig. 2) (14). In the presence of GdnHCl, the band intensity decreased, and the peak wavelength blue shifted to 392 nm, a wavelength typical of free PLP (33). Upon excitation at 298 nm, the emission spectrum of holo-OASS was centered at 340 nm (Fig. 3*a*) (21). In the presence of increasing concentrations of GdnHCl, the emission band progressively shifted to the red and increased in intensity. For the apoenzyme, the emission intensity (excitation at 298 nm) was almost 2-fold that of the holoenzyme due to the absence of the energy transfer to the coenzyme (21). The emission intensity decreased at low denaturant concentrations, and the band shifted toward the red, whereas at higher denaturant concentrations, the emission intensity was found to increase (Fig. 3*b*). At a concentration of GdnHCl higher than about 2 M, the emission of apo- and holoenzyme were very similar, as also indicated by the dependence of the emission maximum on denaturant concentration (Fig. 3*c*). The fluorescence increase of the apoenzyme was due to the direct effect of denaturant on tryptophan emission properties (34),

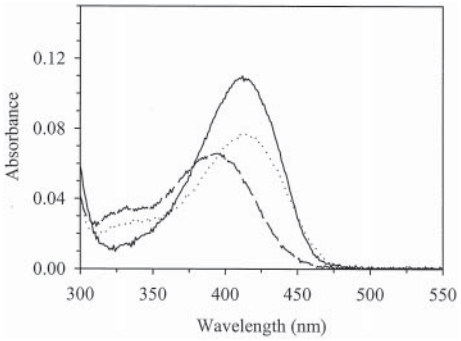

FIG. 2. **Absorption spectra of holo-OASS in the absence and presence of 4.0 M GdnHCl.** A solution of the native enzyme (15.4 μM) in 100 mM Hepes, pH 7, was mixed with an equal volume of a solution containing 100 mM Hepes, 8.0 M GdnHCl, pH 7. Absorption spectra were recorded in the absence (*continuous line*) and in the presence of the denaturant after 1 min (*dotted line*) and after 60 min (*dashed line*).

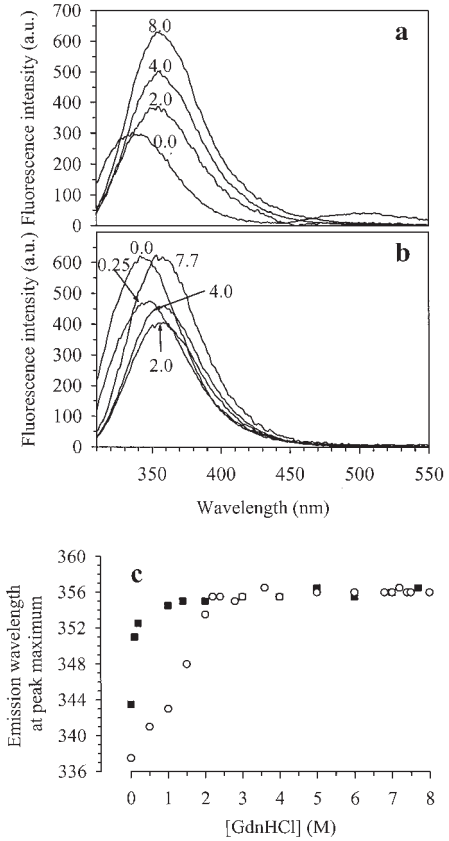

FIG. 3. **Effect of denaturation on the emission spectra of holo-OASS (*a*) and apo-OASS (*b*) upon excitation at 298 nm ($slit_{ex}$ = 2.5 nm; $slit_{ex}$ = 2.5 nm).** Emission spectra were recorded under equilibrium conditions in the absence and presence of different molar concentrations of GdnHCl (indicated in the figure). Data are normalized to the same enzyme concentration, 3.5 μM protomers, 100 mM Hepes, pH 7, at 20 °C. *c*, dependence of the peak wavelength for holo- (*open circles*) and apo-OASS (*closed squares*) as a function of GdnHCl concentration. *a.u.*, arbitrary units.

whereas the fluorescence increase of holoenzyme on denaturant concentration was likely due to a combination of two effects: the decrease of energy transfer between tryptophan and coenzyme (21) and the influence of denaturant on tryptophan emission, as also observed for the apoenzyme.

The difference emission spectra between the folded and unfolded enzyme exhibited a maximum value at 363.5 and 326.5 nm for holo- and apo-OASS, respectively (data not shown). The fluorescence emission intensities at these wavelengths were

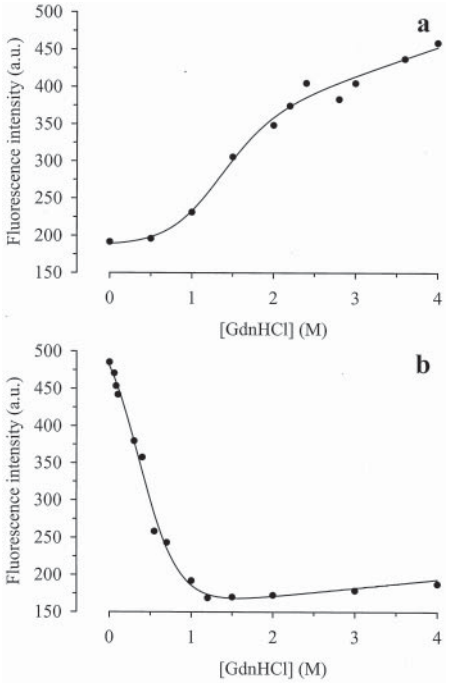

FIG. 4. **Dependence of the fluorescence emission intensity of holo-OASS at 363.5 nm (*a*) and apo-OASS at 326.5 nm (*b*) on denaturant concentration (λ_{ex} = 298 nm).** The *solid lines* represent the fitting of the data to a two-state model according to Equation 5. The linear extrapolation method (26) (Equations 1–4) has been preferred in the determination of the thermodynamic parameters since it resulted in more accurate values. The transition midpoints and the unfolding free energies are 1.57 ± 0.15 and 2.72 ± 0.40 kcal/mol and 0.47 ± 0.02 and 1.47 ± 0.11 kcal/mol for holo- and apoenzyme, respectively. *a.u.*, arbitrary units.

plotted as a function of GdnHCl concentration (Fig. 4, *a* and *b*). A 10-fold change of protein concentration (0.35–3.5 μM) was not found to affect the dependence of fluorescence emission intensity on the denaturant concentration (data not shown).

Time-resolved Fluorescence and Fluorescence Anisotropy—A three-exponential process was used to describe tryptophan fluorescence intensity decays of holo- and apoenzyme upon excitation at 295 nm (21). The detailed analysis of tryptophans and coenzyme lifetime decays as a function of denaturant concentration will be reported elsewhere.[2] The rotational correlation times and their respective fractions, as obtained from the enzyme intrinsic tryptophan fluorescence anisotropy decays, are shown as a function of GdnHCl concentration in Fig. 5. The two distinct rotational correlation times, ϕ_1 and ϕ_2, were assigned to the slow protein tumbling and the fast local motion of the fluorophores (28, 35). The limiting anisotropy was fixed to r_0 = 0.29, which is consistent with values expected for tryptophan (36). The faster rotational correlation time, attributed to the intrinsic motion of the probe, exhibited similar values for the holo- and apoenzyme and was consistent with the expected values for the rotation of indolyl side chains of Trp (37). Within the experimental error, no appreciable dependence on denaturant concentration was observed for the fast motion. The slower rotational rate, which provides information on the global and structural motions of the protein, strongly decreased as a function of GdnHCl concentration, reaching a practically constant value at about 2.5 and 1.5 M for the holo- and apo-OASS, respectively.

The internal aldimine fluorescence intensity decays, upon excitation of the bound coenzyme at 454.5 nm, were well fit by a double exponential decay model (20).[2] The total fluorescence intensity drops sharply with the increase of GdnHCl concentration, and reliable measurements could not be carried out above 2.0 M due to the release of PLP (see "Discussion"). The coenzyme anisotropy decays were fit to a single macromolecular species having two associated rotational correlation times (Fig. 6). The shortening of the longer rotational correlation time at increasing denaturant concentrations was less pronounced than that observed through the tryptophan anisotropy decays. Notably, the relative fractions were unaffected by the presence of GdnHCl in the measured range. This characteristic was closely tied to the presence of bound PLP (see "Discussion").

^{31}P NMR Experiments on PLP, PLP-valine Methyl Ester Schiff Base, and OASS in the Absence and Presence of Guanidinium Chloride—^{31}P NMR experiments were carried out for PLP, PLP-valine methyl ester Schiff base, and holo-OASS in the absence and presence of 0.8 and 2.0 M GdnHCl (Table I). The signal of free PLP is at 3.86 ppm in the absence of GdnHCl and shifts downfield to 4.53 ppm in the presence of 2.0 M GdnHCl. This effect was probably due to the considerable increase in ionic strength (a similar behavior was observed in the presence of 2.0 M NaCl; data not shown). For the model, Schiff base in the absence of denaturant two ^{31}P signals were observed at 3.68 and at 3.30 ppm. In the presence of 2 M GdnHCl, the signals shift downfield to 4.54 and 4.21 ppm. In contrast, the OASS signal shifted upfield from 5.13 to 4.54 and 4.13 ppm, with the 4.54-ppm signal predominant in the presence of denaturing agent. The signal at 4.54 ppm indicated some free PLP, whereas the signals at lower ppm (4.21 and 4.13 ppm for PLP-valine methyl ester and OASS, respectively) were interpreted as the model aldimine in the presence of denaturant.

Far UV Circular Dichroism Spectra—Under native conditions, the mean residue ellipticity was significantly lower in the apo- than in the holoenzyme (Fig. 7, *a* and *b*). CD spectra of the holo- and apoenzyme, collected in the presence of GdnHCl under equilibrium conditions, showed a gradual reduction of the ellipticity (Fig. 7, *a* and *b*). A small negative signal was still present at 6.0 M GdnHCl (Fig. 7*c*), suggesting that even at this high denaturant concentration the protein is locally structured. A 10-fold change of protein concentration (1.5–15 μM) did not affect the dependence of ellipticity on GdnHCl concentration (data not shown).

Dynamic Light-scattering Measurements—The diffusion coefficient of OASS is reported in Fig. 8 as a function of GdnHCl concentration in the range 0–3.5 M. The diffusion coefficients were corrected for the solution viscosity, although this does not change the data appreciably, amounting to a maximum correction of 10% at [GdnHCl] ≅ 1.5 M. The measured diffusion coefficient showed a smooth decrease up to about 1 M denaturant, whereas at higher concentrations the diffusion coefficient showed a steep decrease corresponding to a ≅50% increase in the protein size at 1.5 M GdnHCl. The mean value of the diffusion coefficient obtained for [GdnHCl] < 0.2 M, D = 70.3 ± 0.5 μm^2/s, was consistent with a dimeric form of the protein. In fact, we estimated $D_{monomer}$ = 85 μm^2/s, and D_{dimer} = 69 μm^2/s for the diffusion coefficient of the monomer and dimer forms of OASS, respectively, assuming a monomer molecular weight of 34,450 dalton, a partial molecular volume v = 0.78 ml/g (38), and adding a water shell of ≅0.28 nm. A correction for the shape anisotropy of the OASS dimer, an oblate ellipsoid with the short axes of about 4.5 nm and the longest axis of about 8.5 nm (Protein Data Bank 1OAS), was found to be minimal, a≅ 3% increase of the dimer diffusion coefficient, and did not change the good agreement between the theoretical value and our experimental findings.

DISCUSSION

The far UV CD spectra collected in native conditions (Fig. 7, *a* and *b*) exhibit a different composition of secondary structure

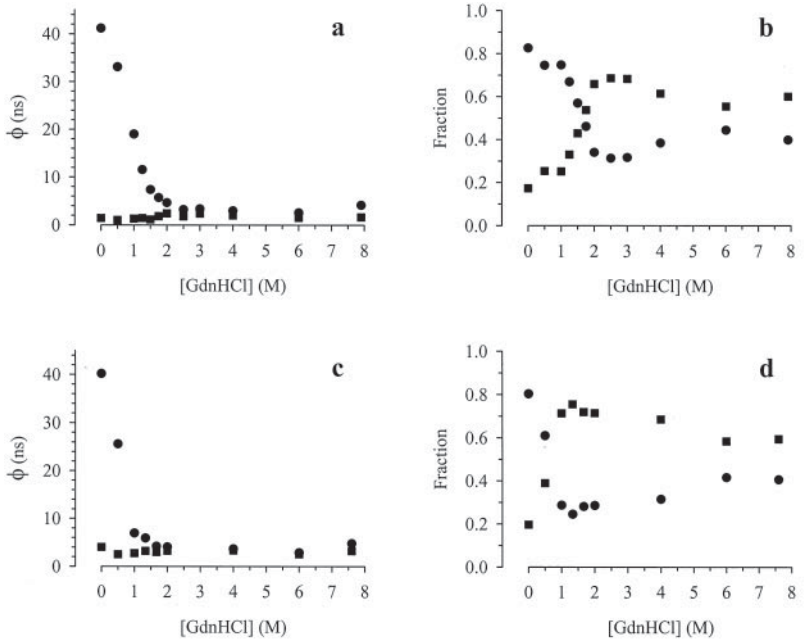

FIG. 5. **Rotational correlation times of tryptophans as a function of GdnHCl concentration upon excitation at 295 nm.** Holo-OASS rotational correlation times (*a*) and the corresponding anisotropy fractions (*b*) were calculated from anisotropy decays measured for solutions containing 9.65 μM protomers, 100 mM Hepes, pH 7, 20 °C. Each sample was equilibrated for 24 h at the desired GdnHCl concentration, 20 °C. Apo-OASS rotational correlation times (*c*) and the corresponding anisotropy fractions (*d*) were measured under the same solution conditions used for the holoenzyme, at 4.80 μM protomers concentration. Each point is the best fit to 2–7 separate experiments (global $\chi^2 < 5.0$). For clarity, the ϕ values for the shorter rotational correlation time (*squares*) have been multiplied 10-fold.

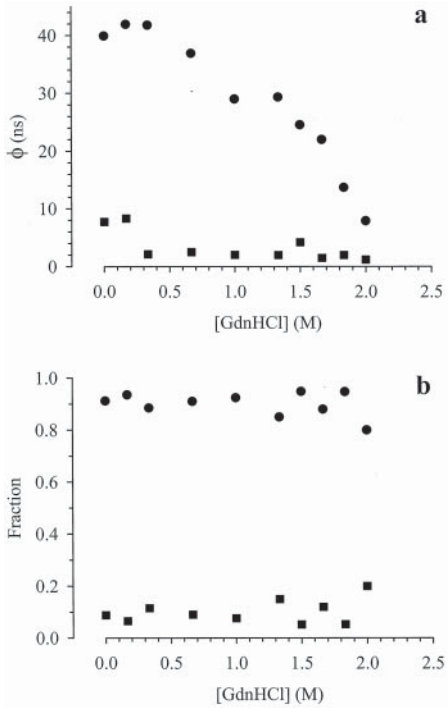

FIG. 6. **GdnHCl dependence of PLP fluorescence anisotropy decays upon excitation at 454.5 nm.** The rotational correlation times (*a*) and the corresponding fractions (*b*) were measured on solutions containing 19.3 μM holo-OASS, 100 mM Hepes, pH 7, 20 °C after equilibration for 24 h at variable GdnHCl concentration. Each point is the best fit to 2 to 4 separate experiments (reduced global $\chi^2 < 1.0$). For clarity, the reported ϕ values of the shorter rotational correlation time (*squares*) have been multiplied 10-fold.

TABLE I
^{31}P NMR of PLP, PLP-valine methyl ester Schiff base, and holo-OASS in the absence and presence of GdnHCl at pH 7.0

Species	GdnHCl	ppm
	M	
PLP	0.0	3.86
	0.8	4.37
	2.0	4.53
PLP-valine methyl ester	0.0	3.68 3.30 (+)[a]
	0.8	4.36 3.95 (+)[a]
	2.0	4.54 4.21 (+)[a]
PLP-OASS	0.0	5.13
	2.0	4.54 (+)[a] 4.13

[a] The + indicates that this peak has a higher intensity.

elements for apo- compared with holo-OASS. In contrast, other PLP-dependent enzymes, including serine hydroxymethyltransferase (39, 40), mitochondrial aspartate aminotransferase (41) (fold type I), and tryptophan synthase (42) (fold type II), exhibit similar spectra for the apo- and holoenzyme. Despite the well known uncertainty in the quantitative evaluation of secondary structure content from CD spectra, the calculated values for holo-OASS are in good agreement with the crystallographic data (Table II). On the basis of the circular dichroism data, the native apoenzyme exhibits a lower helical content than the holoenzyme and an increased amount of β structures. The inspection of the three-dimensional structure of the holo enzyme (5) indicates that both tryptophans are located in α-helical segments. As shown by fluorescence measurements (Fig. 3), following the re-organization of the secondary structure, Trp residues are more solvent-exposed in native apo-OASS (maximum at 343 nm) than in holo-OASS (maximum at 338 nm) (43). In holo-OASS, phosphorescence studies (18) indicate that Trp-161 is embedded in a more polar environment than Trp-50. Conformational changes associated with the binding of the coenzyme and the preferential quenching of Trp-50 emission due to energy transfer to PLP (18, 21) account for a different contribution of the two residues to the total emission of holo- and apoenzyme.

Unfolding of holo-OASS leads to an increased average distance between tryptophans and coenzyme and a reorientation of the corresponding transition dipole moments, hampering the energy transfer and increasing tryptophan fluorescence quantum yield. Moreover, the increased solvent exposure of tryptophan residues in the denatured state is the origin of the shift of the emission maximum to 355 nm.

The GdnHCl dependence of the tryptophan emission in holo- and apo-OASS (Fig. 4) indicates that protein regions where the tryptophans are localized are more stable when PLP is bound, as shown by the different denaturation mid-points. These findings demonstrate not only that the coenzyme strongly increases the protein stability, but also that, even in the absence of denaturant, the presence of the PLP is necessary to attain

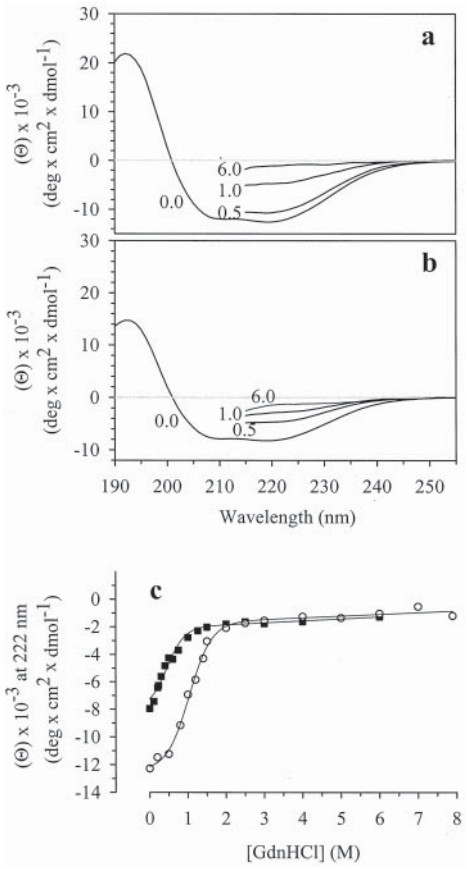

FIG. 7. **Far UV circular dichroism spectra of OASS as a function of GdnHCl concentration.** CD spectra of holo- (*a*) and apo-OASS (*b*) were recorded for enzyme solutions containing 20 mM phosphate, pH 7.0, at 20 °C in the absence and presence of different GdnHCl concentrations (indicated in the figure). *c*, dependence on GdnHCl concentration of the mean residue ellipticity at 222 nm for holo- (*open circles*) and apo-OASS (*closed squares*). The *solid lines* are the fits to Equation 5. The thermodynamic parameters have been calculated using the linear extrapolation method (26) (Equations 1–4), yielding more accurate values. The transition midpoints and the unfolding free energies are 1.03 ± 0.03 and 2.05 ± 0.15 kcal/mol and 0.39 ± 0.02 and 1.58 ± 0.17 kcal/mol for holo- and apo-OASS, respectively.

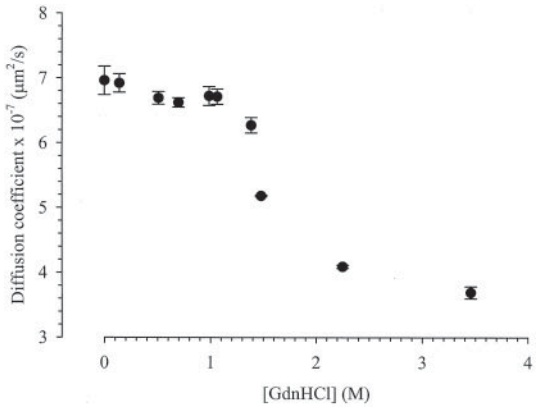

FIG. 8. **Mutual diffusion coefficient *D* of holo-OASS as a function of GdnHCl concentration.** The reported data are corrected for the solution viscosity.

the correct native fold. The stabilizing effect of the coenzyme was also reported for glutamate decarboxylase (44), aspartate aminotransferase (41, 45–48), sheep liver serine hydroxymethyltransferase (40), tryptophanase (49–51) (fold type I), and tryptophan synthase (52–54) (fold type II) but not in *Escherichia coli* serine hydroxymethyltransferase (39) and DOPA decarboxylase (55) (fold type I). On the basis of this limited enzyme set, it would appear that the stabilizing role of the coenzyme is not strictly associated with the fold type.

TABLE II
Secondary structure content of native holo- and apo-OASS

	α-Helix	β-Sheet	Others
	%	%	%
Holo-OASS[a]	34.8	15.2	50.0
Holo-OASS[b]	37.0	14.0	45.6
Apo-OASS[b]	28.7	22.9	52.1

[a] Values obtained from the crystallographic data (Protein Data Bank file 1OAS) (5).

[b] Values obtained from the deconvolution of far-UV CD spectra with the CD Spectra Deconvolution software, Version 2.1 (65). Since the fractions of different secondary structure elements are computed separately, with a 3.5% tolerance, the sum of the calculated fractions is slightly different from 100% (96.6 and 103.7% for holo- and apo-OASS, respectively).

The equilibrium unfolding curves of holo-OASS, as calculated from the denaturant dependence of the ellipticity at 222 nm (Fig. 7*c*), are significantly right-shifted compared with those obtained by monitoring tryptophan fluorescence (Fig. 4*a*). This result suggests that either the N- or the C-terminal domain of the OASS monomer is endowed with higher stability than the overall protein. Although the coenzyme is located at the interface between the domains, it makes different contacts with the N- and C-terminal domain. The phosphate group of PLP interacts with the positive dipole of the N terminus of helix 7 and makes several hydrogen bonds with residues Gly-176, Thr-177, Gly-178, and Thr-180 in the loop between strand 7 and helix 7 of the C-terminal domain (5). These bonds could lead to a higher stability of the C-terminal domain, containing Trp-161, with respect to the N-terminal domain, containing Trp-50. The latter domain is more quenched through energy transfer by the coenzyme and would be expected to contribute more to the change in fluorescence, which occurs upon unfolding.

The overlapping of the denaturation curves for apo-OASS, as monitored by tryptophan fluorescence (Fig. 4*b*) and circular dichroism (Fig. 7*c*), strengthens the interpretation that the two structural domains of holo-OASS are differentially stabilized by the interaction with the coenzyme. The stabilizing effect of PLP on OASS is not evident above 2 M GdnHCl, where the denaturation curves for holo- and apo-OASS are superimposable (Figs. 4 and 7). To understand whether this is simply due to the disruption of the network of interactions between the coenzyme and the protein matrix or to the breakage of the Schiff base and the consequent release of the PLP, the dependence of the absorption and ^{31}P NMR spectra of the coenzyme in the presence of denaturant was measured. Upon exposure of the holo-OASS to high concentrations of GdnHCl, the intensity of the 412-nm band first decreases without any spectral shift (Fig. 2). This transient species exhibits spectral properties and NMR signals similar to those of model PLP amino acid Schiff bases (33) and is attributed to the presence of coenzyme still bound to the denatured enzyme. This state slowly converts into a new species that absorbs at lower wavelengths (Fig. 2) and is typical of free PLP (33). The ^{31}P NMR signal of the phosphate group of OASS-bound PLP shows an upfield shift upon exposure to 2 M GdnHCl from 5.13 to 4.54 ppm (Table I). An upfield shift was also observed after an open to close conformational transition when native OASS forms an external aldimine with L-serine (14). However, as indicated by the absorption data and by the observation that free PLP and OASS in the presence of denaturant exhibit the same peak at 4.54 ppm, the most likely explanation for the observed behavior is the breakage of the covalent bond between the PLP and the side chain of Lys-41.

Moreover, the release of the coenzyme could account for the sharp decrease of the internal aldimine fluorescence intensity at 500 nm in the presence of denaturant, which is almost completely suppressed at 2.0 M GdnHCl.

The dependence of the anisotropy decays on denaturant (Fig. 5) also indicates that the almost complete unfolding of holo- and apo-OASS occurs at about 2.0 and 1.0 M GdnHCl, respectively. In the absence of denaturant, the longer rotational correlation time is about 40 ns, independent of the intrinsic fluorescence probe (Trp or coenzyme) and the presence of PLP (Figs. 5 and 6). The expected rotational correlation time for a roughly spherical protein of 69,000-Da molecular mass at 20 °C is approximately 30 ns (Ref. 56 and references therein). The slightly higher value attained, 40 ns, can be explained by the oblate ellipsoid shape of this enzyme and the imprecise knowledge of its solution hydration state and specific volume. The low relative contribution of local motions is consistent with the fact that both tryptophans are embedded in a relatively rigid environment, as suggested by the low B factors, determined crystallographically (29.7 and 24.6 $Å^2$ for Trp-50 and Trp-161, respectively) (5). Such behavior is even more evident in the coenzyme anisotropy decays (Fig. 6). The faster rotational correlation time of tryptophans is relatively insensitive to the GdnHCl concentration (Fig. 5), but their respective anisotropy amplitudes are not. The speed of the fast local motion of the tryptophans would not necessarily be expected to increase significantly upon protein denaturation since the local motion is normally fast, even in the native protein. The fractional amplitude of the fast rotational correlation time, however, increases as unfolding proceeds since it pertains to the scope of the tryptophan motion and not its speed. In the intact protein, the tryptophan motion is hindered by the organized protein structure. When the protein structure is loosened, the freedom of the tryptophan motion increases, as clearly signaled (Fig. 5). Upon unfolding, the increased flexibility of the polypeptide chain prevents the fluorescent probes to track the global motions of the protein. The shortening of the slow rotational correlation time and its lower relative contribution to the anisotropy decay as a function of denaturant concentration reflect the increasing weight of segmental motions. The apparent convergence of the fractions of the slow and fast components observed at higher denaturant concentrations is a consequence of the fact that the more the two rotational correlation times approach each other, the more difficult it is to discriminate the two populations, which ultimately tend to merge (57).

The fluorescence anisotropy data suggest that monomer formation does not take place before denaturation. Furthermore, the transition midpoints of the denaturation curves obtained from fluorescence and circular dichroism data did not exhibit any measurable dependence on protein concentration when the latter was varied in a 10-fold range (data not shown). The monomerization as a function of denaturant concentration was specifically addressed by dynamic light-scattering experiments on the holo-OASS (Fig. 8). The results indicate that a relatively modest increase in the average radius accompanies the conformational events that lead to the loss of most of the native tertiary and secondary structure. Thus, the strong interface interactions prevent the (partially) unfolded dimer from assuming largely expanded conformations. The sharp increase in the size of the molecule observed at denaturant concentrations higher than the transition midpoint for unfolding is due to further unfolding of the monomer once the interface constraints are loosened or lost. Accordingly, no significant change of the average radius is observed between 0.5 and 1.0 M GdnHCl, a range of concentration that is in the steep region of the denaturation curve, as monitored by fluorescence and circular dichroism, because of the compensating effect of monomerization and monomer expansion.

The resulting mechanism for OASS-unfolding requires that most of the native secondary structure is disrupted after the release of the coenzyme, but strong intermonomer interactions force the protein to maintain a relatively compact, although flexible, conformation according to anisotropy data. Once the structure is sufficiently destabilized, monomerization occurs, leading to a further expansion of the isolated monomers, although there is evidence for some degree of structural organization (native or non-native), even at the higher denaturant concentrations. This is suggested by the small but significant negative ellipticity observed at 210–220 nm in the presence of 6 M GdnHCl (Fig. 7, *a* and *b*) and is in agreement with the behavior of tryptophans lifetime decays.[2] The apparent two-state behavior and the absence of protein concentration dependence of equilibrium unfolding arise from the very high degree of structural destabilization required to allow the monomerization, so that no intermediate states having spectroscopic properties significantly different from the native dimer or the unfolded monomer are populated at equilibrium.

Different mechanisms of unfolding have been proposed for other PLP-dependent proteins on the basis of equilibrium and kinetic data. In DOPA decarboxylase (55), *E. coli* aspartate aminotransferase (48, 58, 59) (fold type I), and alanine racemase (60) (fold type III) no appreciable loss of secondary structure takes place before monomerization.

Steady-state fluorescence equilibrium curves, when analyzed according to Equations 1–4 (see "Materials and Methods"), yield unfolding free energies of 2.72 ± 0.40 and 1.47 ± 0.11 kcal/mol for holo- and apoenzyme, respectively. Despite significantly different midpoints (see Figs. 4 and 7), similar $\Delta G_{0,U}$ values, 2.05 ± 0.15 and 1.57 ± 0.17 kcal/mol, are found when far UV circular dichroism is used to monitor unfolding. The calculated free energies should not be considered as absolute values because of the approximation to a two-state system. The unusually strong intermonomer interactions require that a high degree of unfolding has to be achieved to allow monomerization, so that fluorescence and circular dichroism are no longer sensitive to the last monomerization/unfolding events, and the contribution of intersubunit interactions to the overall stability is probably underestimated. Moreover, some residual structural organization under denaturing conditions might affect the estimate of the unfolding $\Delta G_{0,U}$ by contributing to the native state stability (61), However, the calculated thermodynamic parameters should represent good estimates and suggest that the free energies of stabilization for apo- and holo-OASS are low when compared with other proteins of comparable size. Furthermore, the slow unfolding rate ($\tau_{1/2}$ is of the order of several hours at low denaturant concentration) suggests that kinetics compensate for the modest thermodynamic stability by minimizing the probability of the protein to sample unfolded or partially folded states. Kinetic stability as a mechanism for longevity has been suggested for α-lytic protease (62, 63), an extracellular bacterial protease.

It has been suggested (64) that the marginal stability of the native state of proteins arises from the balance between two fundamental requisites: a well defined three-dimensional structure, required for functional specificity, and an adequate flexibility to allow the conformational changes associated with ligand binding, catalysis, and allosteric regulation. The three-dimensional structure of the methionine external aldimine of a K41A mutant of OASS from *S. typhimurium* has been recently reported (15). The external aldimine structure is in a closed conformation, demonstrating that ligand binding induces very large local and global conformational changes in OASS. In this

perspective, it might be interesting to determine if, and to what extent, the stabilizing effect of the coenzyme varies in different catalytic intermediates. Furthermore, in the case of OASS, one more level of conformational flexibility is required for reversible binding and reciprocal regulation by serine acetyltransferase in the cysteine synthase multienzyme complex.

Acknowledgments—We are extremely grateful to Dr. Paul F. Cook, University of Oklahoma, Norman, OK for providing us *O*-acetylserine sulfhydrylase A-isozyme and for helpful discussion. Circular dichroism experiments were performed at the Centro Interdipartimentale Misure of the University of Parma.

REFERENCES

1. Alexander, F. W., Sandmeier, E., Mehta, P. K., and Christen, P. (1994) *Eur. J. Biochem.* **219,** 953–960
2. Grishin, N. V., Phillips, M. A., and Goldsmith, E. J. (1995) *Protein Sci.* **4,** 1291–1304
3. Schneider, G., Kack, H., and Lindkvist, Y. (2000) *Structure* (*Lond.*) **8,** 1–6
4. Hyde, C. C., Ahmed, S. A., Padlan, E. A., Miles, E. W., and Davies, D. R. (1988) *J. Biol. Chem.* **263,** 17857–17871
5. Burkhard, P., Rao, G. S. J., Hohenester, E., Schnackerz, K. D., Cook, P. F., and Jansonius, J. N. (1998) *J. Mol. Biol.* **283,** 121–133
6. Kredich, N. M., and Tomkins, G. M. (1966) *J. Biol. Chem.* **241,** 4955–4965
7. Kredich, N. M., Becker, M. A., and Tomkins, G. M. (1969) *J. Biol. Chem.* **244,** 2428–2439
8. Becker, M. A., Kredich, N. M., and Tomkins, G. M. (1969) *J. Biol. Chem.* **244,** 2418–2427
9. Cook, P. F., and Wedding, R. T. (1978) *J. Biol. Chem.* **253,** 7874–7879
10. Hindson, V. J., Moody, P. C. E., Rowe, A. J., and Shaw, W. V. (2000) *J. Biol. Chem.* **275,** 461–466
11. Cook, P. F., and Wedding, R. T. (1977) *Arch. Biochem. Biophys.* **178,** 293–302
12. Rege, V. D., Kredich, N. M., Tai, C.-H., Karsten, W. E., Schnackerz, K. D., and Cook, P. F. (1996) *Biochemistry* **35,** 13485–13493
13. Christen, P., and Metzler, D. E., eds (1985) *Transaminases*, John Wiley & Sons, Inc., New York
14. Schnackerz, K. D., Tai, C.-H., Simmons, J. W., Jacobson, T. M., III, Rao, G. S. J., and Cook, P. F. (1995) *Biochemistry* **34,** 12152–12160
15. Burkhard, P., Tai, C.-H., Ristroph, C. M., Cook, P. F., and Jansonius, J. N. (1999) *J. Mol. Biol.* **291,** 941–953
16. Mozzarelli, A., Bettati, S., Pucci, A. M., Burkhard, P., and Cook, P. F. (1998) *J. Mol. Biol.* **283,** 135–146
17. McClure, G. D., and Cook, P. F. (1994) *Biochemistry* **33,** 1674–1683
18. Strambini, G. B., Cioni, P., and Cook, P. F. (1996) *Biochemistry* **35,** 8392–8400
19. Benci, S., Vaccari, S., Mozzarelli, A., and Cook, P. F. (1997) *Biochemistry* **36,** 15419–15427
20. Benci, S., Vaccari, S., Mozzarelli, A., and Cook, P. F. (1999a) *Biochim. Biophys. Acta* **1429,** 317–330
21. Benci, S., Bettati, S., Vaccari, S., Schianchi, G., Mozzarelli, A., and Cook, P. F. (1999b) *J. Photochem. Photobiol. B Biol.* **48,** 17–26
22. Hara, S., Payne, M. A., Schnackerz, K. D., and Cook, P. F. (1990) *Protein Expression Purif.* **1,** 79–90
23. Tai, C.-H., Nalabolu, S. R., Jacobson, T. M., Minter, D. E., and Cook, P. F. (1993) *Biochemistry* **32,** 6433–6442
24. Schnackerz, K. D., and Cook, P. F. (1995) *Arch. Biochem. Biophys.* **324,** 71–77
25. Bradford, M. (1976) *Anal. Biochem.* **72,** 248–254
26. Pace, C. N. (1986) *Methods Enzymol.* **131,** 266–280
27. Beechem, J. M., and Gratton, E. (1988) *SPIE* **909,** 70–78
28. Weber, G. (1977) *J. Chem. Phys.* **66,** 4081–4091
29. Steiner, R. F. (1991) in *Topics in Fluorescence Spectroscopy* (Lakowicz, J. R., ed) pp. 1–52, Plenum Publishing Corp., New York
30. Chirico, G., and Gardella, M. (1999) *Appl. Opt.* **38,** 2059–2067
31. Nozaki, Y. (1972) *Methods Enzymol.* **26,** 43–50
32. Kawahara, K., and Tanford, C. (1966) *J. Biol. Chem.* **241,** 3228–3232
33. Kallen, R. G., Korpela, T., Martell, A. E., Matsushima, Y., Metzler, C. M., Metzler, D. E., Morozov, Y. V., Ralston, I. M., Savin, F. A., Torchinsky, Y. M., and Ueno, H. (1985) in *Transaminases* (Christen, P., and Metzler, D. E., eds) pp. 37–108, John Wiley & Sons, Inc., New York
34. Eftink, M. R. (1994) *Biophys. J.* **66,** 482–501
35. Jameson, R. M., and Hazlett, T. L. (1991) in *Biophysical And Biochemical Aspects Of Fluorescence Spectroscopy* (Dewey, D. G., ed) pp. 105–133, Plenum Publishing Corp., New York
36. Weber, G. (1960) *Biochem. J.* **75,** 335–345
37. Munro, I., Pecht, I., and Stryer, L. (1979) *Proc. Natl. Acad. Sci. U. S. A.* **76,** 56–60
38. Tanford, C. (1961) *Physical Chemistry of Macromolecules*, John Wiley and Sons, Inc., New York
39. Cai, K., Schirch, D., and Schirch, V. (1995) *J. Biol. Chem.* **270,** 19294–19299
40. Venkatesha, B., Udgaonkar, J. B., Rao, N. A., and Savithri, H. S. (1998) *Biochim. Biophys. Acta* **1384,** 141–152
41. Artigues, A., Iriarte, A., and Martinez-Carrion, M. (1994) *J. Biol. Chem.* **269,** 21990–21999
42. Balk, H., Merkl, I., and Bartholmes, P. (1981) *Biochemistry* **20,** 6391–6395
43. Lakowicz, J. R. (1983) *Topics in Fluorescence Spectroscopy*, pp. 241–277, Plenum Publishing Corp., New York
44. Chen, C.-H., Wu, S. J., and Martin, D. L. (1998) *Arch. Biochem. Biophys.* **349,** 175–182
45. Ivanov, V. I., Bocharov, A. L., Volkenstein, M. V., Karpeisky, M. Y., Mora, S., Okina, E. I., and Yudina, L. V. (1973) *Eur. J. Biochem.* **40,** 519–526
46. Relimpio, A., Iriarte, A., Chlebowski, J. F., and Martinez-Carrion, M. (1981) *J. Biol. Chem.* **256,** 4478–4488
47. Reyes, A. M., Iriarte, A., and Martinez-Carrion, M. (1993) *J. Biol. Chem.* **268,** 22281–22291
48. Herold, M., and Kirschner, K. (1990) *Biochemistry* **29,** 1907–1913
49. Raibaud, O., and Goldberg, M. E. (1973) *J. Biol. Chem.* **248,** 3451–3455
50. Skrzynia, C., London, J., and Goldberg, M. E. (1974) *J. Biol. Chem.* **249,** 2325–2326
51. Mizobata, T., and Kawata, Y. (1995) *J. Biochem.* (*Tokyo*) **117,** 384–391
52. Zetina, C. R., and Golberg, M. E. (1980) *J. Biol. Chem.* **255,** 4381–4385
53. Seifert, T., Bartholmes, P., and Jaenicke, R. (1985) *Biochemistry* **24,** 339–345
54. Remeta, D. P., Miles, E. W., and Ginsburg, A. (1995) *Pure Appl. Chem.* **67,** 1859–1866
55. Dominici, P., Moore, P. S., and Borri Voltattorni, C. (1993) *Biochem. J.* **295,** 493–500
56. Hazlett, T. L., Moore, K. J. M., Jameson, D. M., and Eccleston, J. F. (1993) *Biochemistry* **32,** 13575–13583
57. Mei, G., Rosato, N., Silva, N., Jr., Rusch, R., Gratton, E., Savini, I., and Finazzi-Agro, A. (1992) *Biochemistry* **31,** 7224–7230
58. Herold, M., and Leistler, B. (1992) *FEBS Lett.* **308,** 26–29
59. Leistler, B., Herold, M., and Kirschner, K. (1992) *Eur. J. Biochem.* **205,** 603–611
60. Toyama, H., Esaki, N., Tanizawa, K., and Soda, K. (1991) *J. Biochem.* (*Tokyo*) **110,** 279–283
61. Neet, K. E., and Timm, D. E. (1994) *Protein Sci.* **3,** 2167–2174
62. Cunningham, E. L., Jaswal, S. S., Sohl, J. L., and Agard, D. A. (1999) *Proc. Natl. Acad. Sci. U. S. A.* **96,** 11008–11014
63. Sohl, J. L., Jaswal, S. S., and Agard, D. A. (1998) *Nature* **395,** 817–819
64. Jaenicke, R. (1991) *Eur. J. Biochem.* **202,** 715–728
65. Böhm, G., Muhr, R., and Taenicke, R. (1992) *Protein Eng.* **5,** 191–195